RSC Advances

PAPER

Cite this: *RSC Adv.*, 2021, **11**, 5055

Biodegradable calcium carbonate/mesoporous silica/poly(lactic-glycolic acid) microspheres scaffolds with osteogenesis ability for bone regeneration

Weikang Xu, †‡*abc Ruifang Zhao,†a Tingting Wu,a Guixiang Li,a Kun Wei*c and Liyan Wang*d

Received 24th November 2020
Accepted 18th January 2021

DOI: 10.1039/d0ra09958a

rsc.li/rsc-advances

Sintered microsphere-based scaffolds provide a porous structure and high-resolution spatial organization control, show great potential for bone regeneration, mainly from biodegradable biomaterials including poly(lactic-glycolic acid) (PLGA). However, acidic monomer regeneration, mainly from biodegradable biomaterials including poly(lactic-glycolic acid) (PLGA). However, acidic monomers generated by PLGA degradation tend to cause tissue inflammation, which is the central issue of PLGA-based bone regeneration scaffolds development. In this work, calcium carbonate (CC)/hexagonal mesoporous silica (HMS)/PLGA sintered microsphere-based scaffolds were developed. The scaffolds possessed a three-dimensional (3D) network structure and 30–40% porosity. The degradation results indicated that CC/HMS/PLGA scaffolds could compensate for pH increased caused by PLGA acidic byproducts effectively. Degradation results showed that CC/HMS/PLGA scaffold could effectively compensate for the pH increase caused by PLGA acidic by-products. Composite CC additives can induce the increase of adhesive proteins in the environment, which is conducive to the adhesion of cells to scaffolds. Mesenchymal stem cells (MSCs) proliferation and osteogenic differentiation were evaluated by CCK-8 assay, alkaline phosphatase (ALP) activity, ALP staining, and Alizarin Red staining. The results showed that compared with HMS/PLGA scaffolds, the proliferation of MSCs cultured with CC/HMS/PLGA scaffolds was enhanced. When cultured on the CC/HMS/PLGA scaffolds, MSCs also showed significantly enhanced ALP activity and higher calcium secretion compared with the HMS/PLGA scaffolds. CC/HMS/PLGA sintered microsphere-based scaffolds provides an attractive strategy for bone repair and regeneration with better performance.

1. Introduction

Due to trauma, infections, tumors, and other causes, millions of patients suffer from bone defects every year, most of which are difficult to repair, which presents a challenge to clinical orthopedics worldwide.[1] At present, the main solution is to use autograft or allograft.[2] However, the successful application of these bone grafts has been limited by local hematoma, vascularization problems, and bone tissue integration in the host.[3] In order to repair bone defects successfully, tissue engineering requires the development of new bone graft materials based on scaffolds, cells and growth factors.[4]

Scaffolds play an important role in bone repair and regeneration, for they provide a mechanical architecture that induces the growth of cultured cells.[5] Microspheres have long been used in drug delivery applications due to their excellent controlled release ability.[6] And also, its shape is rigid and can form porous three-dimensional (3D) structures, either alone or in combination with other materials, to be a scaffold for tissue engineering.

[a]*Department of Scientific Research, National Engineering Research Center for Healthcare Devices, Guangdong Key Lab of Medical Electronic Instruments and Polymer Material Products, Guangdong Institute of Medical Instruments, Institute of Health Medicine, Guangdong Academy of Sciences, No. 1307 Guangzhou Avenue Central, Tianhe District, Guangzhou, Guangdong 510500, China. E-mail: 759200816@qq.com; Tel: +86-757-87-02-35-80*

[b]*Guangdong Provincial Bioengineering Institute (Guangzhou Sugarcane Industry Research Institute), Guangdong Academy of Sciences, Jianghai Avenue Central, Haizhu District, Guangzhou, Guangdong 510316, China*

[c]*National Engineering Research Center for Human Tissue Restoration and Function Reconstruction, South China University of Technology, Wushan Road 381, Guangzhou, Guangdong 510006, China. E-mail: 3084786673@qq.com; Tel: +86-757-39-38-00-98*

[d]*Department of Stomatology, Foshan Woman and Children's Hospital, No. 11 Renmin Xi Road, Chancheng District, Foshan, Guangdong 528000, China. E-mail: wangliyankmmc@163.com; Tel: +86-757-82-96-97-89*

† These authors contributed equally to this work.

‡ Present address: No. 1307 Guangzhou Avenue Central, Tianhe District, Guangzhou, Guangdong, 510500, China.

Scaffolds with microsphere preparation techniques have attracted much attention and can be roughly divided into microsphere-incorporating scaffolds and microsphere-based scaffolds.[7] Microsphere-incorporating scaffolds have several advantages over conventional bulk scaffolds, including spatial–temporal control of drug release and enhanced structural or mechanical properties. However, microsphere-incorporating scaffolds are typically prepared in multiple steps using a top-down approach, while microspheres are only part of it. Which presents challenges in the control of cell infiltration and viability in the scaffold matrix, clinical management, and drug delivery.[8,9] To overcome the disadvantage of the top-down approach, a bottom-top method of making microsphere-based scaffolds based on the microsphere itself has become increasingly popular. The microsphere-based scaffolds can be divided into the injectable scaffold and sintered scaffold. Injectable microsphere-based scaffolds, such as PLGA-based scaffolds, are liquid suspensions that can obtain the shape of defects after implantation.[10,11] They may be easy to migrate from the defect sites after implantation due to weak interparticle interactions.[8] However, the sintered microsphere-based scaffolds are made into a specific shape by agglomerating individual microspheres. As a result, these scaffolds are not limited to leakage from the defect when implantation. In addition, sintered microsphere-based scaffolds can be implanted into the body through a special delivery device arthroscopy.[12]

Many studies involving sintered microsphere-based scaffolds have verified their biocompatibility[13,14] and tissue regeneration potential.[15,16] As one of the most widely used synthetic polymers in the preparation of bone regeneration scaffolds, poly(lactic-*co*-glycolic acid) (PLGA) is a biodegradable polymer with excellent processing ability, which can prepare the flexible structure and has a customized degradation rate.[17,18] However, PLGA lacks cell-affinitive moieties and its degradation products are acidic and mechanical strength is poor, which limits its application in the clinic.

Hybridization of PLGA with inorganic biomaterial to improve mechanical strength is a direct and simple modification method. Inorganic materials can be calcium phosphate cement, hydroxyapatite (HA), bioactive glass, and mesoporous silica.[19–21] Silicon, a ubiquitous environmental element, plays an important role in the metabolism of connective tissue, especially bone.[22] Hexagonal mesoporous silica (HMS) is a typical silicon-based material with good physical properties.[23] In the previous study, we chose HMS to hybridize with PLGA, which effectively improved the compressive strength of the PLGA scaffold.[14] However, compared with PLGA scaffolds, the degradation rate and cytocompatibility of HMS/PLGA scaffold had not been significantly improved. Calcium carbonate (CC) is an important part of natural shells, which has good biocompatibility and degradability, which can delay the degradation of PLGA membrane and maintain a good pH value.[24,25] *In vivo*, it forms a close interface with new bone.[26] Studies have shown that corals composited of CC have similar osteogenic properties as HA. Artificial CC porous ceramics have also been proved to have good biocompatibility and guide bone regeneration.[27] Although HA is a widely studied inorganic material for bone repair, the degradation rate of synthetic HA is too slow, and the degradation rate of the material substrate may not match the tissue growth rate. Compared with HA, CC has better biodegradability.[28–30] However, to our knowledge, HMS/CC/PLGA sintered microsphere-based scaffolds have not been reported for bone tissue engineering to date.

In this study, we propose that by introducing CC into HMS/PLGA sintered microsphere-based scaffolds, CC can react with the acidic degradation products from PLGA, so as to ease the overall degradation rate of HMS/PLGA sintered microsphere-based scaffolds, and have a positive effect on the scaffolds' overall cytocompatibility and osteogenic activity. Biocompatibility and osteogenic capacity are assessed using mesenchymal stem cells (MSCs). This work will lead to the design of bone tissue regeneration scaffolds with better performance.

2. Materials and methods

2.1 Materials

Ethyl alcohol (EtOH) and dichloromethane were purchased from Chemical Reagent Factory (Guangzhou, China). Calcium carbonate was purchased from Aladdin Chemistry Co. Ltd (Shanghai, China). Poly(lactic-*co*-glycolic acid) with a ratio of lactic to glycolic acid monomer units of 50 : 50 was purchased from Daigang Biomaterials (Jinan, China). This copolymer has an average molecular weight of 31 000 g mol^{-1} with an intrinsic viscosity of 0.30 dl g^{-1} in chloroform at 30 °C. Polyvinyl alcohol (PVA) was obtained from Sigma-Aldrich (Singapore). Reagents for cell-culture were purchased from Gibco (Carlsbad, CA, USA). CCK-8 was produced in Dojindo, (Kumamoto, Japan).

2.2 Preparation of PLGA and HMS/PLGA microspheres scaffolds

HMS was based on traditional techniques.[14,31] CC/HMS/PLGA microspheres were prepared by a single emulsion solvent evaporation method. Briefly, 1 g of PLGA, 0.15 g of HMS particles, and CC (0.1 and 0.3 g) were dissolved in 8 ml of dichloromethane, mixing was taken in 2 min. The synthetic mixture was then injected with 0.8% PVA solution and stirred for 10 h, allowing the solvent to evaporate completely. CC/HMS/PLGA microspheres were separated and rinsed with deionized water 5 times.

HMS/PLGA and CC/HMS/PLGA sintered microsphere-based scaffolds were poured HMS/PLGA and CC/HMS/PLGA microspheres into cylindrical molds, which were then sintered at 70 °C for 2 h.

2.3 SEM analysis

The morphology of sintered microsphere-based scaffolds was characterized by scanning electron microscopy (SEM, 30XLFEG, Philips, The Netherlands).

2.4 Density and porosity determination

The density and porosity of sintered microsphere-based scaffolds were determined by the method described in ref. 32. Briefly, take ethanol as the liquid phase and keep it at 25 °C. A

bottle full of ethanol weighed W_1. Placing the sample of scaffolds (cylindrical bracket, 10 mm in diameter and 20 mm in height, weighed W_S) into the bottle, ethanol with the same volume of the sample overflowed. The bottle full of the rest of the ethanol and the placed sample weighed W_2. ρ is the density of ethanol at 25 °C. The porosity (P) and density (D) are calculated as follows:

$$D = W_S/((\pi \times R^2) \times H) \quad (1)$$

$$P = 1 - ((W_1 - W_2 + W_S)/\rho)/((\pi \times R^2) \times H) \quad (2)$$

2.5 Compressive testing

Cylindrical scaffolds ($n = 6$) with a length to diameter ratio of 2 : 1 (10 mm in length and 5 mm in diameter) were used for compressive testing. Compressive testing to failure was conducted using an Instron mechanical testing machine (Instron model 5544, Canton, MA) with a crosshead speed of 5 mm min^{-1} at ambient temperature and humidity. The maximum compressive strength of scaffolds was determined using Merlin software associated with the Instron machine.

2.6 Degradation studies

The cylindrical sintered microsphere-based scaffolds (diameter = 10 mm) were weighed and then soaked in a bottle containing 10 ml PBS (pH = 7.4). All bottles were incubated at 37 °C. The wet weight and dry weight of the samples were measured. The pH of the degrading medium was determined by an acidometer (Schott Instruments, Germany). The mass loss and water uptake of the scaffolds were calculated as follows:

$$\text{Weight loss (\%)} = 100 \times [1 - (M_{dry}/M_0)] \quad (3)$$

$$\text{Water uptake (\%)} = 100 \times [(M_{wet} - M_{dry})/M_0]$$

where M_0 and M_t are the initial mass and the mass after t day's immersion, respectively.

2.7 Static contact angles

CC and HMS particles were mixed with a solution containing 2 g PLGA and 10 ml dichloromethane at a weight ratio of 0 : 1.5 : 10 or 3 : 1.5 : 10 or 1 : 1.5 : 10 CC to HMS to PLGA. Swirl the mixture until a uniform suspension is formed, then pour it into the glass dish. Subsequently, CC/HMS/PLGA composite film was removed after complete evaporation of the solvent. The static contact angles of HMS/PLGA and CC/HMS/PLGA films (1 × 1 cm) were determinated by a contact angle analyzer (First Ten Ǻvngstroms, Virginia, USA) using sessile drop technique. The measurements were made at room temperature using deionized water as probe liquid. Droplets of 25 microliters are deposited on the sample surface at a rate of 5 μL s^{-1} through a gauge dispensing needle. Each contact angle reported here is the average of at least five measurements, and the contact angles were determined by the direct optical image of the camera.

2.8 Protein adsorption

First, HMS/PLGA and CC/HMS/PLGA scaffolds (100 mg) were placed in 150 μg ml^{-1} bovine serum albumin (BSA/PBS) solution (500 μL) or Dulbecco's modified Eagle's medium (DMEM) with 10% (v/v) fetal bovine serum (FBS) on an oscillator (25 rpm) for 6 h, respectively.[33] After rinsing thoroughly with PBS, the scaffolds were homogenized with 1% sodium dodecyl sulfate solution and then centrifuged at 48 °C for 15 min. Total protein in the supernatant was quantified by Bradford Reagent assay (Sigma-Aldrich, USA) and MicroBCA™ protein assay (Pierce, Rockford, IL).

2.9 Cell culture on sintered microsphere-based scaffolds

MSCs were purchased from American type cultured specimens (ATCC, Manassas, VA). The scaffolds used for cell research *in vitro* (diameter = 10 mm, height = 5 mm) were sterilized by soaking in 70% ethanol for 24 h, rinsed with PBS for 3 times for 30 min, and exposed to UV light on each side for 30 min. The cells were inoculated on the sintered microsphere-based scaffolds at a density of 1×10^5 cells per scaffold. The cells were cultured in DMEM supplemented with 10% FBS. The cell morphology on the scaffolds was characterized by Quanta 200 SEM. After 2 days of culture, the scaffolds were washed with PBS and fixed at 2.5% glutaraldehyde at 4 °C for 24 h. The scaffolds were then dehydrated for 10 min with a series of graded ethanols (50%, 70%, 80%, 90%, 95%, and 100%) and then freely dried.

2.10 Cell proliferation

Cell proliferation of all scaffolds was quantitatively analyzed by CCK-8 assay. Briefly, the culture medium was removed and the cells were washed twice with PBS (pH = 7.2), at a specified interval. CCK-8 solution was added to each well and incubated in the incubator for 2 h. The absorbance was measured at 450 nm with a microplate reader (Thermo3001, America).

2.11 Osteogenic differentiation

Scaffolds with cells were cultured in osteogenic medium (OGM) to study the osteogenic differentiation of cells. Alkaline phosphatase (ALP) activity was determined by pNPP assay (*p*-nitrophenyl phosphate liquid substrate, Sigma Diagnostics). Briefly, the scaffolds with cells were prewashed with PBS, and then the adherent MSCs were removed from the scaffolds and lysed at 4 °C for 10 min in 0.5 ml PBS containing 0.1 M glycine, 1 mM $MgCl_2$, and 0.05% Triton X-100. The dissolved products of *p*-nitrophenyl phosphate (pNPP) are incubated in solutions at 37 °C for 30 min. To extract the cells layer, the cells were sonicated twice for 30 s and centrifuged at 12 300 rpm for 2 min at 4 °C. The supernatant detects ALP activity, as described earlier.[34] ALP values (U per μg) were normalized to protein content using the Pierce MicroBCA™ Protein Assay Kit (Pierce).

ALP activity of cells on scaffolds was also detected by ALP staining. Briefly, the cultured cells were washed with PBS. And 10% neutral formalin solution fixed for 30 min. The scaffolds with cells were stained with BCIP/NBT dye for 30 min at 37 °C, followed by washing with distilled water.

On the 21st day, alizarin red staining was used to observe the osteogenic mineralization of the cells on the scaffolds. After PBS was rinsed and fixed, alizarin red (40 mM, Sigma) was used for staining at room temperature for 30 min. After rinsing with distilled water several times to remove excess dye, scaffolds were examined under an optical microscope.

2.12 Statistical analysis

The experiment was repeated 3 times, and the results were expressed as mean ± standard deviation. The results were calculated by one-way analysis of variance (one-way ANOVA) and were statistically significant. Tukey test was used for the mean comparison, and statistical significance was defined as $p < 0.05$.

3. Results

3.1 Physical properties of scaffolds

Fig. 1 shows the morphology of HMS/PLGA and CC/HMS/PLGA scaffolds. These scaffolds have a 3D network structure that simulates the natural extracellular matrix structure. The scaffolds were constructed with microspheres, and all types of PLGA-based microspheres remained spherical (Fig. 1, A1, B1 and C1). When the ratio of CC to PLGA increases from 0 to 3 : 10, more CC clumps will enrich the scaffold's surface, thus enhancing their surface roughness (Fig. 1, A2, B2 and C2).

It can be observed that more "humps" appear on the surface of CC/HMS/PLGA sintered microsphere-based scaffolds due to the enrichment of CC and HMS particles, indicating that the addition of CC particles into HMS/PLGA scaffolds increases surface roughness to a large extent. Under the same heat sintering condition, the fusion between sintered microsphere-based scaffolds with higher CC content was poor. As shown in Fig. 1C, there are a large number of HMS and CC dispersion on the CC (30%)/HMS/PLGA surface, and such microspheres are difficult to be fused together.

As shown in Fig. 2, the porosity of these scaffolds is similar (between 30 and 40%). The scaffolds density increased in CC dependence. The densities of CC (10%)/HMS/PLGA and CC (30%)/HMS/PLGA were 0.839 g cm^{-3} and 0.904 g cm^{-3} respectively, which were significantly higher than the 0.783 g cm^{-3} of HMS/PLGA. Because of the worse fusion between microspheres of CC (30%)/HMS/PLGA, the density of CC (30%)/HMS/PLGA was significantly higher than that of CC (10%)/HMS/PLGA scaffolds. When the ratio of CC to PLGA increases from 0 to 1.5 : 10 to 3 : 10, the compressive strength decreased from 16.19 ± 1.34 to 12.54 ± 0.74 to 9.2 ± 0.69 MPa. According to our previous research, we selected the CC (10%)/HMS/PLGA scaffolds for further study. The contact angles of different CC/HMS/PLGA composites decreased significantly, indicating that the addition of CC improved the hydrophilicity of the composites. The contact angle of HMS/PLGA composite surfaces was 63.1 ± 0.2. When the CC content is 0.1 g g^{-1} PLGA, the contact angle was 53.1 ± 0.1.

3.2 Degradation behavior

Fig. 3A shows the weight loss of HMS/PLGA and CC/HMS/PLGA sintered microsphere-based scaffolds. With the progress of the degradation experiment, the weight loss of each group increased. In the five weeks of the degradation experiment, the overall mass loss of the CC/HMS/PLGA group is much lower than that of the HMS/PLGA group. However, in the first week, the mass loss of the CC/HMS/PLGA was higher than the HMS/PLGA. By the fifth week, the mass loss of CC/HMS/PLGA group was 14.8 ± 3.16, while the HMS/PLGA group was 88.0 ± 3.29, which was almost completely degraded.

Fig. 3B shows the change of pH value in the degradation experiment. The pH in both groups decreased slightly during the first 2 weeks. However, the pH value of the CC/HMS/PLGA group fell to around 6.2 after 5 weeks, while the pH value of the HMS/PLGA group was 2.67 after 5 weeks.

3.3 Protein adhesion and cell adhesion

DMEM with 10% FBS and 1% BSA were used to evaluate protein adsorption on scaffolds (Fig. 4). Quantitative measurements showed that all protein quantities in CC/HMS/PLGA were greater than HMS/PLGA.

The adhesion of MSCs to HMS/PLGA and CC/HMS/PLGA scaffolds was shown in Fig. 5. The cells spread and adhere well on both scaffolds, covering the surface of the scaffolds, and the pseudopodia could be clearly seen at large magnification (Fig. 5, A2 and B2), indicating that neither of the two scaffolds had cytotoxicity.

3.4 Cells proliferation

After 1, 3, and 7 days of culture, CCK-8 was used to detect the proliferation of cells in the scaffolds (Fig. 6). The cell proliferation of the CC/HMS/PLGA group was significantly higher than that of the HMS/PLGA group on days 1, 3, and 7. By day 7, CC/HMS/PLGA group showed significant cell proliferation, about 50% higher than HMS/PLGA group.

3.5 Osteogenesis

The cells were cultured in the scaffolds for 3, 7, and 10 days to analyze the ALP content (Fig. 7). The ALP activity of each scaffold increased continuously during the culture period. After 7 and 10 days of culture, the ALP activity of the CC/HMS/PLGA group was significantly higher than that of the HMS/PLGA group. Consistent with the quantitative analysis, direct intracellular ALP staining was performed on the cell layers on day 14, and the staining of the CC/HMS/PLGA group was significantly denser than that of the HMS/PLGA group (Fig. 8, A1 and A2). An important function of osteoblasts is to participate in biomineralization. Calcium deposition of osteoblasts was quantitatively analyzed by alizarin red (Fig. 8, B1 and B2). The results showed that the calcium content secreted by cells on scaffolds increased continuously during the culture period. After 14 days

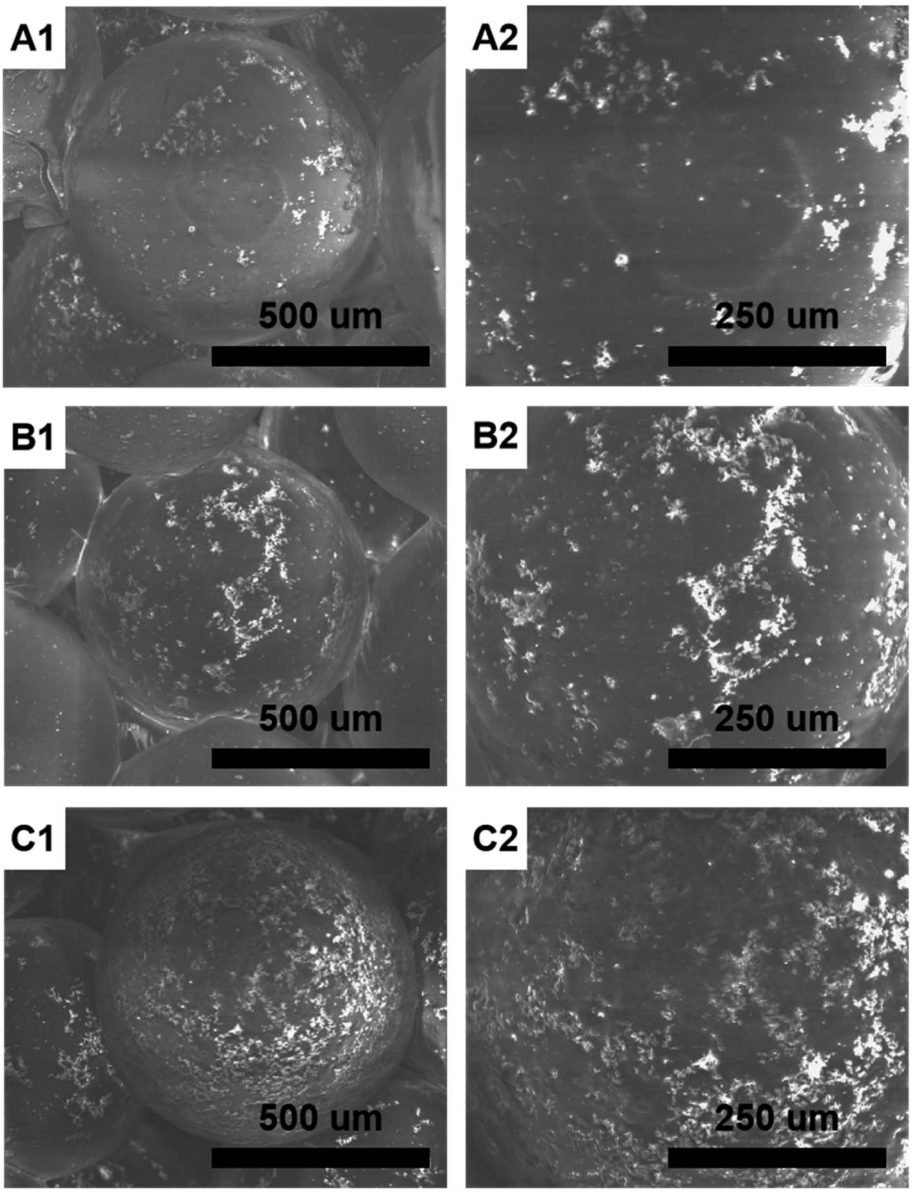

Fig. 1 SEM images of HMS/PLGA (A), CC (10%)/HMS/PLGA (B), and CC (30%)/HMS/PLGA (C) scaffolds.

of culture, the calcium deposition level of the CC/HMS/PLGA group was higher than that of the HMS/PLGA group.

4. Discussion

In this study, CC/HMS/PLGA sintered microsphere-based scaffolds with porous 3D structures, great degradation behavior, and osteogenesis was successfully developed for bone tissue engineering. The adding of CC to HMS/PLGA sintered microsphere-based scaffolds can effectively inhibit its acid degradation. The results of *in vitro* biocompatibility, ALP activity and calcium secretion of MSCs revealed that the CC/HMS/PLGA group could significantly enhance cell proliferation and osteogenesis.

Microspherical-based scaffolds have attracted much attention due to their excellent initial mechanical properties. The sintered microsphere-based scaffolds prepared in this study have a 3D network structure that simulates the structure of the natural extracellular matrix (Fig. 1). And these scaffolds fabricated by heat sintering method possessed 30–40% porosity (Fig. 2), which is consistent with others'.[35] As the ratio of CC to PLGA increased from 1 : 10 to 3 : 10, the enrichment of CC masses on the surface of the scaffold increased, which is due to the agglomeration of CC in the process of emulsification.[36] However, under the same sintering condition, sintered microsphere-based scaffolds with 0.3 g CC per g PLGA had worse fusion between microspheres. At the same time, compared with CC, sheet-shaped HMS may be more advantageous to lock the molecular chain of PLGA, which restricts the movement of PLGA molecular chain in HMS. With the addition of CC, the interlayer locking effect may be weakened []. So that

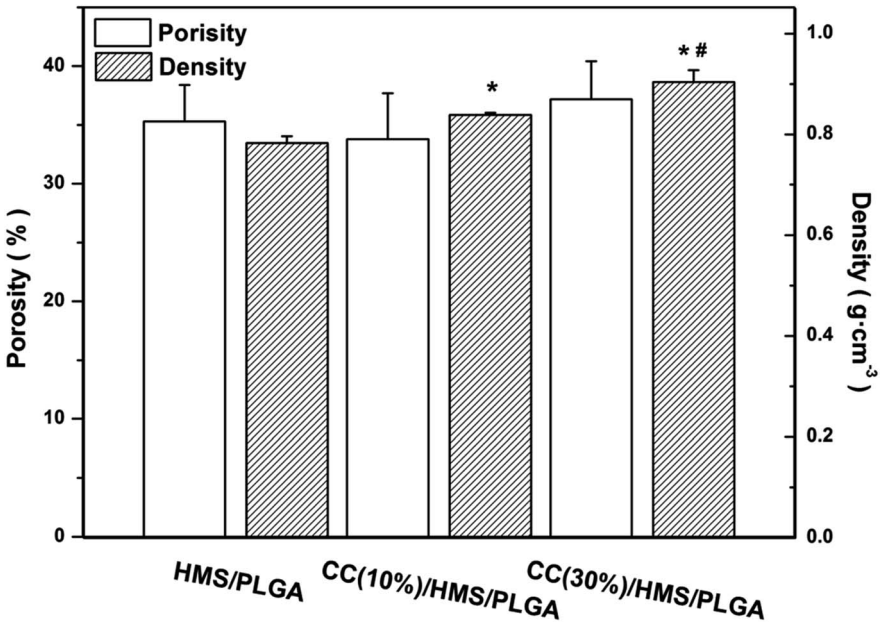

Fig. 2 Porosity and density of HMS/PLGA and CC/HMS/PLGA scaffolds. (*) and (#) showed higher statistical significance compared with HMS/PLGA and CC (10%)/HMS/PLGA, respectively.

the compressive strength of CC/HMS/PLGA is lower than that of the HMS/PLGA.

PLGA has long been approved by the FDA for application in humans. PLGA is considered an ideal polymer for the preparation of tissue engineering materials and drug carrier materials due to its good mechanical properties, biocompatibility, easy molding, and adjustable degradation rate. However, the degradation of PLGA generates acidic monomers, and easy to cause tissue inflammatory reactions and clinic failure is a central issue in the development of PLGA based scaffolds for bone tissue engineering. In this study, as the degradation process progressed, many acidic products from the HMS/PLGA group were dispersed into the medium, resulting in a further decrease in pH value and increased weight loss (Fig. 3). It is well known that the autocatalysis of PLGA may accelerate degradation.[37] For the CC/HMS/PLGA group, CC neutralized acid degradation, so the pH remained above 6 throughout the experiment. In the first week, the weight loss of the CC/HMS/PLGA group was higher than the HMS/PLGA group. This may be due to the better hydrophilicity of CC/HMS/PLGA, PBS is easier to enter the scaffolds, and making them easier to swell and degrade. After the first week, more basic CC was exposed, which neutralized the acidic degradation products of PLGA, thus delaying the degradation of the scaffold.[38] The results

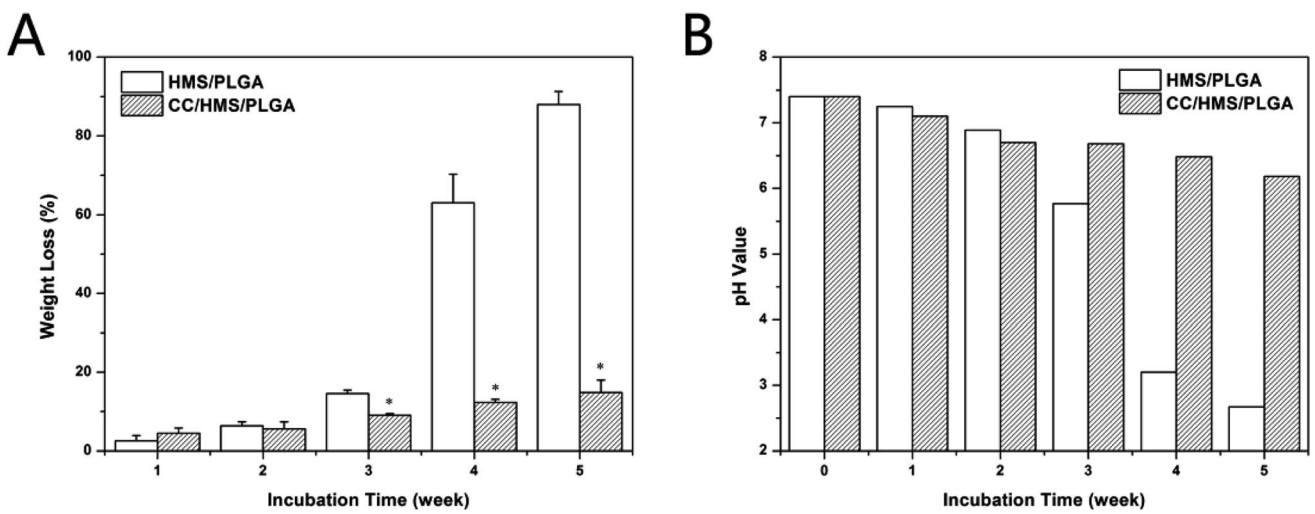

Fig. 3 Weight loss during degradation of HMS/PLGA and CC/HMS/PLGA scaffolds (A). pH change of PBS solution during degradation of HMS/PLGA and CC/HMS/PLGA scaffolds (B).

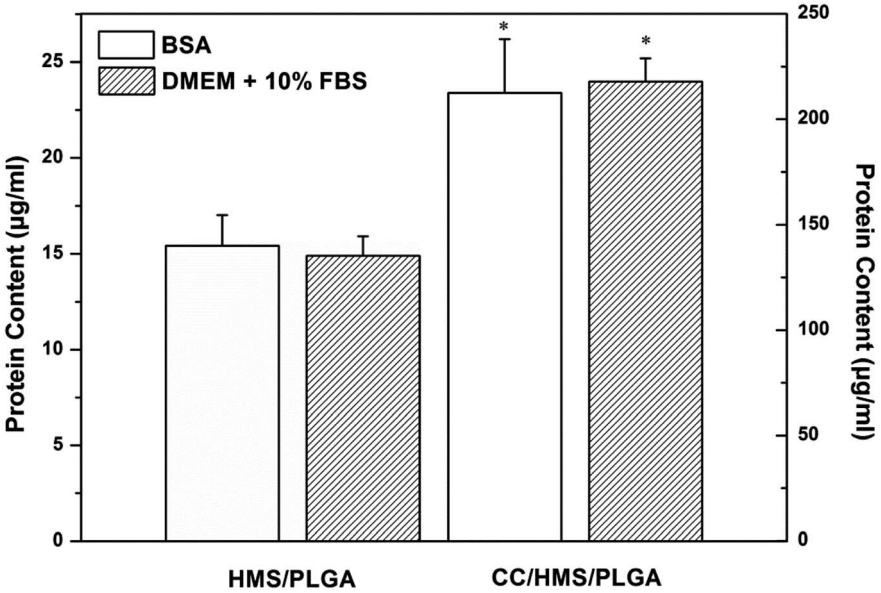

Fig. 4 Human FBS and BSA were adsorbed on the HMS/PLGA and CC/HMS/PLGA scaffolds. (*) Statistically significant compared with HMS/PLGA scaffolds.

showed that the introduction of CC could effectively buffer the degradation of HMS/PLGA groups and obtain a more favorable environment, which was conducive to the application of the scaffold *in vivo*.

The adhesion of protein on the sintered microsphere-based scaffolds was further studied. CC containing HMS/PLGA scaffolds absorbed more environmental proteins such as FBS and BSA. It is well known that FBS is rich in multi-adhesion matrix proteins such as fibronectin (FN), which play a key role in cell adhesion through the Arg-Gly-Asp (RGD) sequence.[35] There were statistically significant differences in cell adhesion between HMS/PLGA and CC/HMS/PLGA, suggesting that PLGA, HMS, and CC particles composite scaffolds promoted MSCs adhesion (Fig. 5). It can be concluded from the results of protein absorption and cell adhesion experiments that the increase of cell adhesion to the CC-containing scaffolds are mainly due to

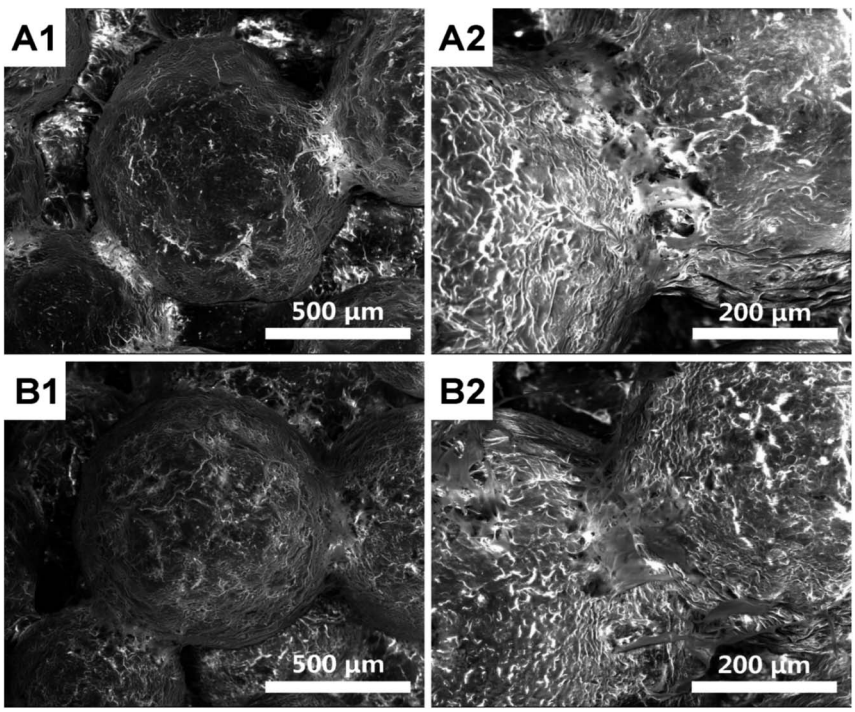

Fig. 5 SEM images of MSCs on the surface of HMS/PLGA (A) and CC/HMS/PLGA (B) scaffolds after 2 days of culture.

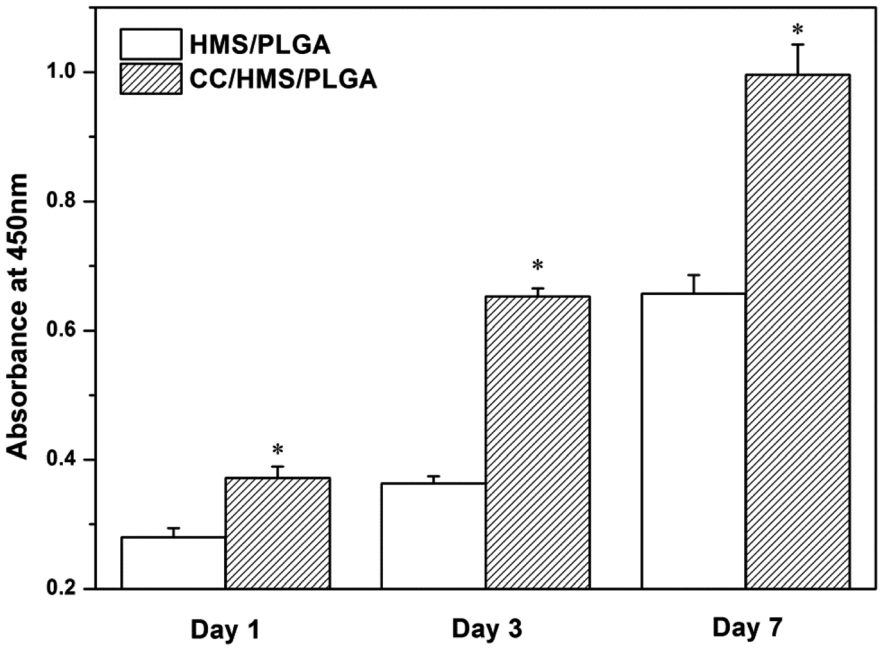

Fig. 6 The proliferation of MSCs was detected by CCK-8. (*) The comparison with HMS/PLGA scaffolds was statistically significant ($p < 0.05$).

the scaffolds capturing more functional proteins, such as FN, from the environmental media before cell contact. In addition to improving the degradation performance of HMS/PLGA scaffolds, CC also plays an active role in improving the biocompatibility of scaffolds. The results of the CCK-8 experiment (Fig. 6) showed that the proliferation of MSCs on CC-containing scaffolds was significantly higher than that on CC-free scaffolds. CC increases protein absorption and subsequent MSCs adhesion. This is consistent with reports that CC/PLGA scaffolds promote human osteosarcoma cell attachment and proliferation.[38]

ALP is an early marker of osteogenic differentiation and mineralization is considered as a late marker of osteogenic differentiation. ALP, mainly expressed on the cell surface or in stromal vesicles, is an indicator of bone formation and a major regulator of phosphate supplementation in bone

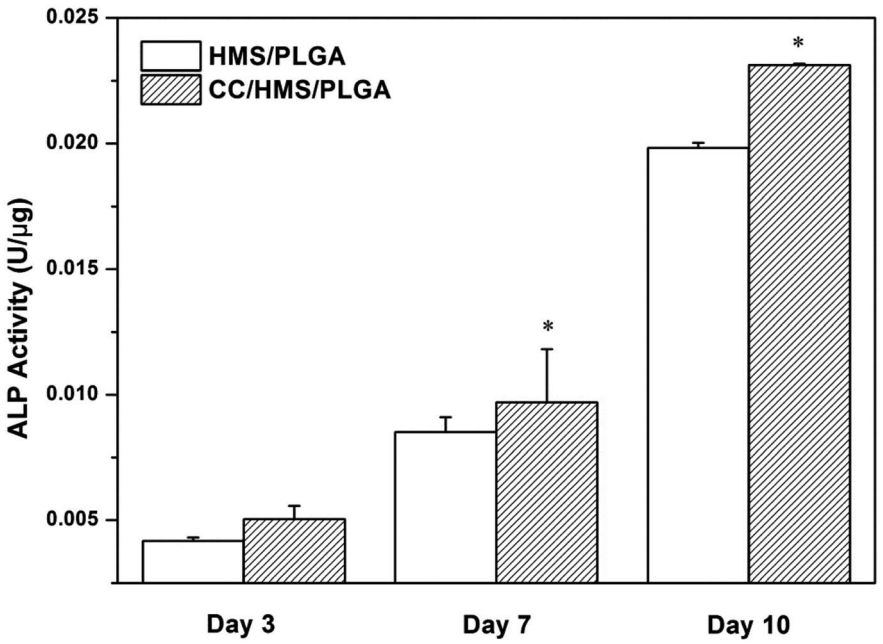

Fig. 7 ALP activity of MSCs was cultured on HMS/PLGA and CC/HMS/PLGA scaffolds for 3, 7, and 10 days. (*) The comparison with HMS/PLGA scaffolds was statistically significant ($p < 0.05$).

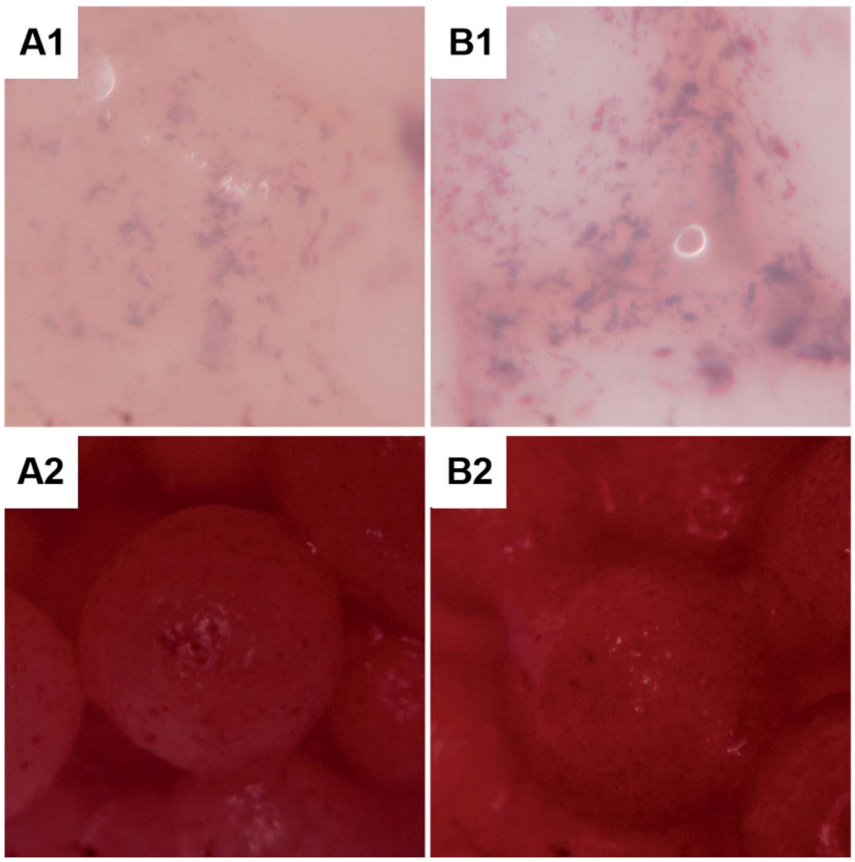

Fig. 8 The MSCs were stained with ALP after 10 days and Alizarin Red after 14 days. MSCs were cultured on HMS/PLGA (A1 and A2) and CC/HMS/PLGA (B1 and B2) scaffolds.

mineralization.[39] ALP activity was significantly increased in CC/HMS/PLGA group (Fig. 7 and 8). Calcium is the main component of the extracellular bone matrix,[40] and the determination of calcium deposition is of great significance for bone formation. In this study, the osteoblasts on CC/HMS/PLGA group also showed significantly higher calcium deposition (Fig. 8). After CC was added to the HMS/PLGA scaffold, MSCs was implanted on the scaffold and expressed osteogenic markers after OGM treatment, indicating that it successfully promoted the osteogenic differentiation of MSCs, which laid a foundation for the development of a PLGA-based 3D porous scaffold containing CC and HMS to promote bone repair.

5. Conclusion

In this study, CC/HMS/PLGA sintered microsphere-based scaffolds were fabricated, which exhibited great degradation properties and cell attachment. In addition, CC/HMS/PLGA sintered microsphere-based scaffolds could effectively enhance MSCs proliferation and osteogenic differentiation. Therefore, CC/HMS/PLGA sintered microsphere-based scaffold is a promising scaffold for bone repair. However, for the bone repair performance of CC/HMS/PLGA scaffolds, more works including animal experiments will be needed to further test.

Conflicts of interest

The authors declare that they have no conflict of interest.

Acknowledgements

This study was supported by the National Natural Science Foundation of China [grant numbers 32000964], Special Fund Project for Guangdong Academy of Sciences to Build First-Class Research Institutions in China [grant numbers 2020GDASYL-20200103038, 2021GDASYL-20210103026, 2019GDASYL-20210102 and 2017GDASCX-0103], Guangdong Province Science and Technology Plan Project [grant numbers 2020B1111560001 and 2017A070701019], Guangzhou Science and Technology Plan Project [grant numbers 201904010280].

References

1 R. Y. Basha, K. T. S. Sampath and M. Doble, *Mater. Sci. Eng., C*, 2015, **57**, 452–463.
2 W. Wang and K. W. K. Yeung, *Bioact. Mater. Med.*, 2017, **4**, 224–247.
3 B. William and M. D. Geissler, *Hand. Clin.*, 2006, **22**, 329–339.

4 T. Winkler, F. A. Sass, G. N. Duda and K. Schmidt-Bleek, *Bone Joint Res.*, 2018, **7**, 232–243.
5 L. G. Griffith and G. Naughton, *Science*, 2002, **295**, 1009–1014.
6 W. Xu, X. Wei, K. Wei, X. Cao and S. Zhong, *Int. J. Pharm.*, 2014, **476**, 116–123.
7 X. Shi, K. Su, R. R. Varshney, Y. Wang and D. A. Wang, *Pharm. Res.*, 2011, **28**, 1224–1228.
8 H. Wang, S. C. G. Leeuwenburgh, Y. Li and J. A. Jansen, *Tissue Eng., Part B*, 2012, **18**, 24–39.
9 J. W. Nichol and A. Khademhosseini, *Soft Matter*, 2009, **5**, 1312–1319.
10 M. J. Chou, C. H. Hsieh, P. L. Yeh, P. C. Chen, C. H. Wang and Y. Y. Huang, *J. Biomed. Mater. Res., Part A*, 2013, **101**, 2862–2869.
11 N. R. Mercier, H. R. Costantino, M. A. Tracy and L. J. Bonassar, *Biomaterials*, 2005, **26**, 1945–1952.
12 A. J. Lozier and D. P. Murphy, *US Pat.*, US8435305 B2, 2014.
13 V. Gupta, K. M. Tenny, M. Barragan, C. J. Berkland and M. S. Detamore, *J. Biomater. Appl.*, 2016, **31**, 328–343.
14 W. Xu, L. Wang, Y. Ling, K. Wei and S. Zhong, *RSC Adv.*, 2014, **4**, 13495–13501.
15 T. Jiang, Y. Khan, L. S. Nair, W. I. Abdel-Fattah and C. T. Laurencin, *J. Biomed. Mater. Res., Part A*, 2010, **93**, 1193–1208.
16 N. Mohan, V. Gupta, B. P. Sridharan, A. J. Mellott, J. T. Easley, R. H. Palmer, R. A. Galbraith, V. H. Key, C. J. Berkland and M. S. Detamore, *Regener. Med.*, 2015, **106**, 709–728.
17 F. Quaglia, *Int. J. Pharm.*, 2008, **364**, 281–297.
18 A. Giteau, M. C. Venier-Julienne, A. Aubert-Pouëssel and J. P. Benoit, *Int. J. Pharm.*, 2008, **350**, 14–26.
19 W. Xia and J. Chang, *J. Controlled Release*, 2006, **110**, 522–530.
20 M. P. Ginebra, T. Traykova and J. A. Planell, *J. Controlled Release*, 2006, **113**, 102–110.
21 C. Dai, H. Guo, J. Lu, J. Shi, J. Wei and C. Liu, *Biomaterials*, 2011, **32**, 8506–8517.
22 A. Leuchtenberger, *Mol. Nutr. Food Res.*, 2010, **15**, 706.
23 P. T. Tanev and T. J. Pinnavaia, *Science*, 1995, **267**, 865.
24 H. Ohgushi, M. Okumura, T. Yoshikawa, K. Inboue, N. Senpuku, S. Tamai and E. C. Shors, *J. Biomed. Mater. Res., Part A*, 1992, **26**, 885–895.
25 M. Ara, M. Watanabe and Y. Imai, *Biomaterials*, 2002, **23**, 2479–2483.
26 H. Liao, H. Mutvei, M. Sjöström, L. Hammarström and J. Li, *Biomaterials*, 2000, **21**, 457–468.
27 J. Vuola, H. G. Ransson, T. B. Hling and S. Asko-Seljavaara, *Biomaterials*, 1996, **17**, 1761–1766.
28 F. He, J. Zhang, F. Yang, J. Zhu and X. Chen, *Mater. Sci. Eng., C*, 2015, **50**, 257–265.
29 Q. Zhong, W. Li, X. Su, G. Li, Y. Zhou, S. C. Kundu, J. Yao and Y. Cai, *Colloids Surf., B*, 2016, 56–63.
30 N. Yang, Q. Zhong, Y. Zhou, S. C. Kundu, J. Yao and Y. Cai, *Microsc. Res. Tech.*, 2016, **79**, 518–524.
31 P. T. Tanev, M. Chibwe and T. J. Pinnavaia, *Nature*, 1994, **368**, 321–323.
32 Y. Yang, J. Zhao, Y. Zhao, L. Wen, X. Yuan and Y. Fan, *J. Appl. Polym. Sci.*, 2010, **109**, 1232–1241.
33 M. Borden, M. Attawia, Y. Khan and C. T. Laurencin, *Biomaterials*, 2002, **23**, 551–559.
34 L. Zhao, L. Liu, Z. Wu, Y. Zhang and P. K. Chu, *Biomaterials*, 2012, **33**, 2629–2641.
35 M. Borden, M. Attawia and C. T. Laurencin, *J. Biomed. Mater. Res.*, 2002, **61**, 421–429.
36 Y. Wang, X. Shi, L. Ren, Y. Yao, F. Zhang and D. A. Wang, *J. Biomed. Mater. Res., Part B*, 2010, **93**, 84–92.
37 T. Hickey, D. Kreutzer, D. J. Burgess and F. Moussy, *Biomaterials*, 2002, **23**, 1649–1656.
38 D. Cheng, X. Cao, H. Gao and Y. Wang, *RSC Adv.*, 2013, **3**, 6871–6878.
39 H. C. Blair, Q. C. Larrouture, Y. Li, H. Lin and D. J. Nelson, *Tissue Eng., Part B*, 2016, **23**, 268–280.
40 C. Wang, Y. Gong, Y. Zhong, Y. Yao, K. Su and D. A. Wang, *Biomaterials*, 2009, **30**, 2259–2269.